# Unveiling a Novel Insulator-to-Metal Transition in $La_2NiO_{4+\delta}$: Challenging High-Temperature Superconductivity Claimed for Single-Layer Lanthanum Nickelates

Yunqi Ji(吉云奇), Xiaohan Wang(王晓晗), Xiaohe Li(李晓赫), Wenting Tang(唐雯婷), Xinyang Li(李新阳), Xin Wang(王鑫), Fangfei Li(李芳菲)*, Liang Li(李亮)*, and Qiang Zhou(周强)

*Synergetic Extreme Condition User Facility, State Key Laboratory of Superhard Materials, College of Physics, Jilin University, Changchun 130012, China*

(Received 13 May 2024; accepted manuscript online 27 August 2024)

$La_2NiO_4$ has a similar structure to $La_2CuO_4$ and was proposed as a high-temperature superconductor based on magnetic-moment measurements decades ago. Nevertheless, with the exception for electrical resistance drop behavior of about 4 orders of magnitude that is claimed to originate from the superconductivity ever observed in Sr-doped $La_2NiO_4$, most electrical data reported to date in $La_2NiO_4$ system exhibit a trivial insulating ground state. Here, we definitively identify the similar electrical resistance drop behavior of more than 3 orders of magnitude in $La_2NiO_{4+\delta}$. However, our extensive investigations reveal that this phenomenon is a novel insulator-to-metal transition, distinct from superconductivity. Intriguingly, compared to the weak magnetic-field effects, pressure can significantly suppress the transition and transform from the metallic to an insulating ground state, accompanied by an isostructural phase transition. Our work not only elucidates the fundamental properties of the metallic conducting ground state in $La_2NiO_{4+\delta}$, but also critically challenges the notion of superconductivity in single-layer lanthanum nickelates.

DOI: 10.1088/0256-307X/41/9/097402

Since the discovery of superconducting cuprates in the last century, nickelates have received a great deal of attention,[1–3] primarily because Ni is the closest neighbor element of Cu on the periodic table and there are structural similarities between nickelates and cuprates. Through a good deal experimental effort, superconductivity has recently been observed in infinite-layer $LnNiO_2$ (Ln = lanthanide) films,[4–7] obtained by reducing the corresponding $LnNiO_3$ perovskite. However, superconductivity is limited to thin film materials. Very recently, the experimental breakthrough revealed high-$T_c$ superconductivity above liquid-nitrogen temperature in pressurized $La_3Ni_2O_7$,[8–13] belonging to the Ruddlesden–Popper (RP) phase with general formula $La_{n+1}Ni_nO_{3n+1}$ ($n = 2$), which set off a research upsurge on other RP phase nickelates and successfully led to the discovery of superconductivity in $La_4Ni_3O_{10}$ ($n = 3$) under high pressure.[14–17]

As for $La_2NiO_4$ ($n = 1$), due to the structural similarity to the copper-based superconducting parent $La_2CuO_4$,[18–20] its ground state properties have long attracted attention. There have been many reports on the possible high-$T_c$ superconductivity[21–26] in $La_2NiO_4$ systems based on magnetic data. However, except for the electrical resistance drop behavior of about 4 orders of magnitude that is claimed to originate from the superconductivity ever observed in Sr-doped $La_2NiO_4$, most electrical data reported to date in $La_2NiO_4$ system exhibit a trivial insulating ground state.[18,27–30] Hence, it is natural to ask whether this resistance drop exists in undoped $La_2NiO_4$ and whether it arises from superconductivity.

In this work, we synthesized high-quality $La_2NiO_{4.06}$, $La_2NiO_{4.09}$, and $La_2NiO_{4.13}$ single crystals through crucible-free floating-zone technique combined with post-annealing treatment, and reveal a novel insulator-to-metal transition with resistance drop behavior over 3 orders of magnitude. However, based on the lack of both zero-resistance and magnetic-field suppression effects on the transition temperature, we can rule out the possibility of superconductivity in $La_2NiO_{4+\delta}$. Furthermore, we reveal a pressure-induced transition from the metallic ground state to an insulating ground state. Both the transition temperature and transition pressure show a positive dependence on the oxygen content.

Figure 1(a) shows the crystal structure of $La_2NiO_4$. As the first member of RP phase lanthanum nickelates ($n = 1$), $La_2NiO_4$ can be described as the stacking of perovskite blocks ($LaNiO_3$) and rocksalt (LaO) layers along the crystallographic $c$-axis direction. The optical photo of $La_2NiO_4$ single crystals synthesized by the optical floating-zone method is shown in the inset of Fig. 1(d). The length is about 4 cm. The smooth surface reflects a good crystalline quality of the sample. The microscopic crystalline state of the sample was examined using high-resolution transmission electron microscopy (HRTEM) [Fig. 1(b)].

*Corresponding authors. Email: lliang@jlu.edu.cn; lifangfei@jlu.edu.cn
© 2024 Chinese Physical Society and IOP Publishing Ltd

Photos taken along the [1$\bar{1}$0] zone-axis matching well with the theoretical simulation results [the inset in Fig. 1(b)]. The highly ordered atomic arrangement clearly demonstrates the layered structure perpendicular to the $c$-axis and indicates again the good crystalline quality of the sample. The powder x-ray diffraction (XRD) [Fig. 1(c)] confirmed that the sample has a tetragonal structure with a space group of $I4/mmm$. The XRD pattern measured along the crystal growth direction [Fig. 1(d)] has only one peak at 31.4° between 20° and 80°, which can be indexed to the (103) plane. The energy dispersive spectroscopy (EDS) analysis shows the chemical composition is La : Ni = 1.98(4) when setting Ni as 1 (see Fig. S1 in the Supplementary Material), which is very close to the expected stoichiometry within the accuracy of the instrument.

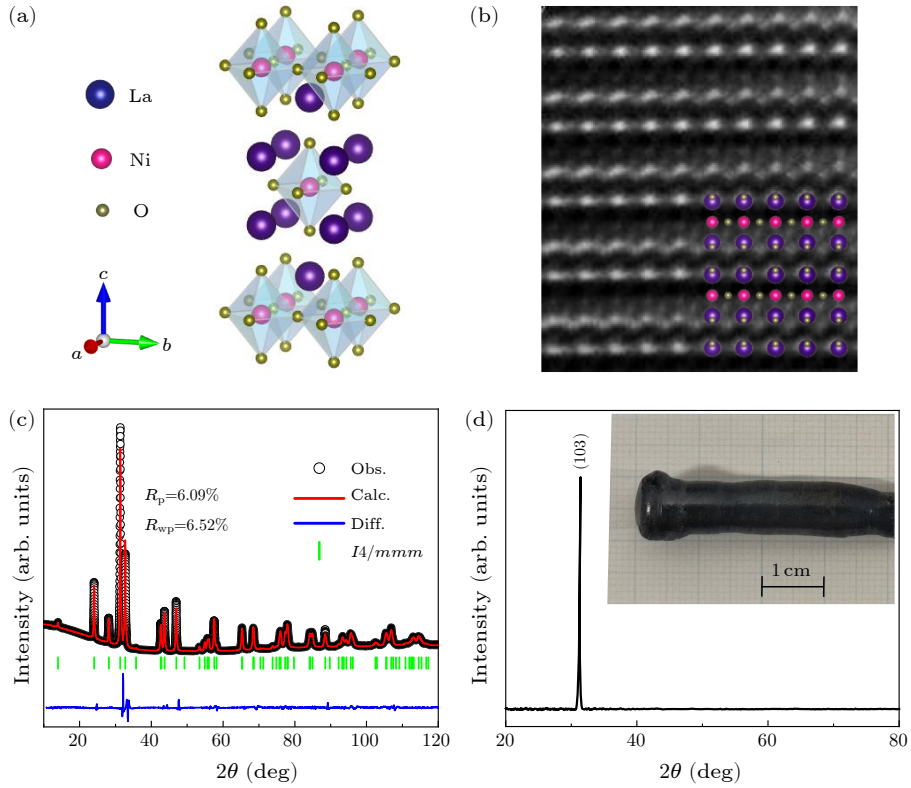


**Fig. 1.** Structural characterization of the as-grown $La_2NiO_{4+\delta}$ single crystals. (a) Illustration of the crystal structure of $La_2NiO_4$ crystal. (b) The HRTEM image of $La_2NiO_{4+\delta}$ along the [1$\bar{1}$0] direction. (c) Rietveld refinement of the x-ray diffraction pattern of pulverized as-grown $La_2NiO_{4+\delta}$ crystals. (d) X-ray diffraction pattern of $La_2NiO_{4+\delta}$ single crystal along the growth direction. The photograph of the as-grown $La_2NiO_4$ single crystals is shown in the upper right inset.

Previous studies have shown that oxygen content has a significant impact on the electrical transport properties of RP phase lanthanum nickelates.[18,30–34] For example, the high-pressure superconductivity of $La_3Ni_2O_7$ and $La_4Ni_3O_{10}$ were only found in samples with specific oxygen content.[32–34] Therefore, we regulated the oxygen content in the single crystals by performing a post-annealing treatment on parts of the as-grown samples under oxidizing and reducing atmospheres ($O_2$ and Ar). The oxygen overstoichiometry $\delta$ in $La_2NiO_{4+\delta}$ annealed in Ar, unannealed, and annealed in $O_2$ determined by iodometry were 0.06, 0.09, and 0.13, respectively. The three specimens are labeled as $La_2NiO_{4.06}$, $La_2NiO_{4.09}$, and $La_2NiO_{4.13}$, respectively, in the following text.

The samples after post-annealing treatment is still single phase with $I4/mmm$ structure (Fig. S2). Figure 2(a) shows the comparison of the peaks corresponding to the (004) and (200) crystal planes in the powder XRD pattern of $La_2NiO_{4+\delta}$. The lattice parameters obtained through refinement are summarized in Fig. 2(b) and Table S1. As the oxygen content increases, the lattice constant $a$ decreases slightly, while the $c$-axis increases significantly, resulting in a net increase in unit-cell volume $V$. The trend of lattice parameters changing with oxygen content is consistent with the previous results.[35,36] Figure 2(c) shows the comparison of the Raman spectra of $La_2NiO_{4+\delta}$. There are two peaks located at 220–225 $cm^{-1}$ and 434–438 $cm^{-1}$, which can be attributed to the apical-oxygen vibration along $a$-axis with the $E_g$ symmetry and along $c$-axis with $A_{1g}$.[37,38] As the oxygen content increases, the peak positions of the two peaks gradually move to low frequencies, and the full width at half maximum (FWHM) gradually becomes larger [Fig. 2(d)]. This could be attributed to the fact that when excess oxygen atoms enter the inter-

layer gap,[20] they will interact with the atoms inside of the layer, resulting in the Ni–O bond in the octahedrons within the layer weaken to varying degrees, and the inconsistency in the strength of the Ni–O bonds is macroscopically reflected in the broadening of the Raman peak. In summary, both XRD and Raman measurements indicate that we have successfully regulated the oxygen content in $La_2NiO_{4+\delta}$.

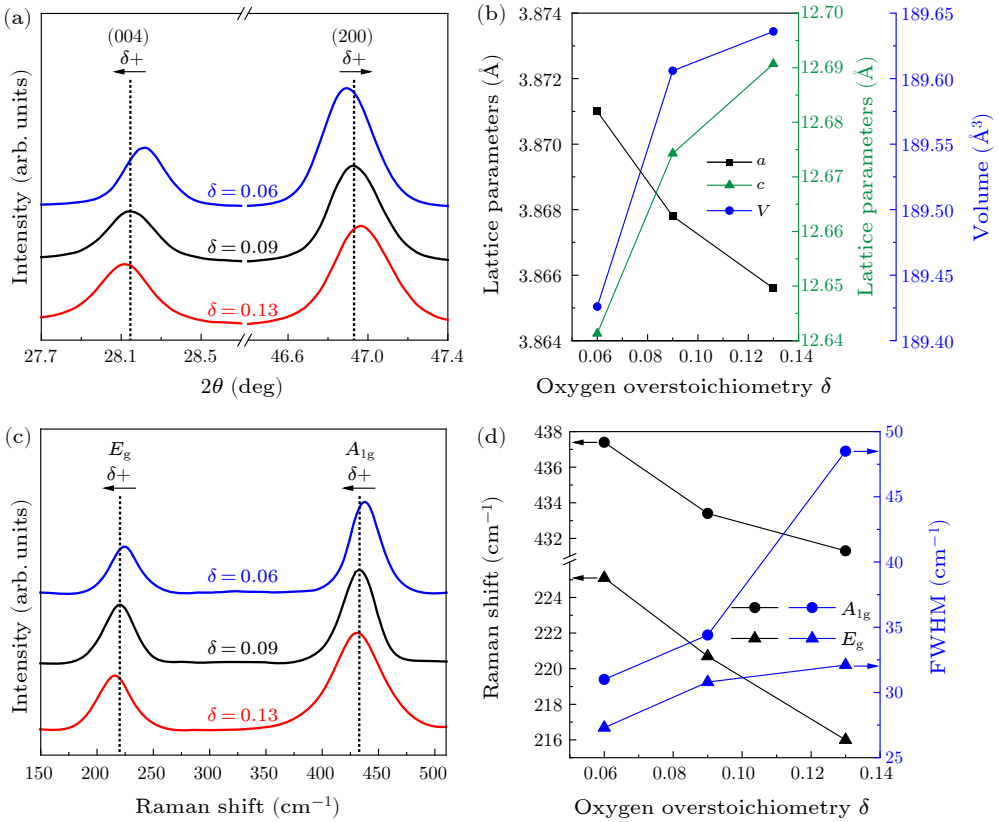


**Fig. 2.** Characterization of the structure and vibrational modes of $La_2NiO_{4+\delta}$ with different $\delta$. (a) Effect of oxygen overstoichiometry $\delta$ on the XRD peaks corresponding to the (004) and (200) crystal plane of $La_2NiO_{4+\delta}$. (b) The obtained lattice parameters and unit-cell volume as a function of oxygen overstoichiometry $\delta$. (c) Effect of oxygen overstoichiometry $\delta$ on the $A_{1g}$ and $E_g$ Raman vibration modes of $La_2NiO_{4+\delta}$. (d) The Raman shift and the full width at half maximum (FWHM) of $A_{1g}$ and $E_g$ vibration modes as a function of oxygen overstoichiometry $\delta$.

After characterizing the composition and structural information of $La_2NiO_{4+\delta}$ samples, we performed electrical transport measurements over the temperature range of 2–300 K on the three samples with different oxygen contents under ambient pressure. The results are shown in Fig. 3(a). Note the overall tendency toward insulating behavior as the temperature is lowered. However, when the temperatures are at 94, 108, and 125 K, accompanied by obvious resistance peaks, the resistance of $La_2NiO_{4+\delta}$ with three oxygen contents suddenly decreases as the temperature decreases, showing metallic conductive characteristics. The transition temperature from insulation to metallic conduction ($T_{IMT}$) increases with the increase in oxygen content, showing a positive dependence. As the temperature continues to decrease, the resistance of $La_2NiO_{4+\delta}$ gradually decreases by more than 3 orders of magnitude to a saturation value, without reaching zero resistance [Fig. 3(b)]. Notably, the similar low-temperature resistance drop behavior has been reported in Sr-doped $La_2NiO_{4+\delta}$ single crystals before,[26] which is claimed to originate from superconductivity ($T_c$ = 25–19 K) combining the magnetic measurement data, whereas the superconductivity has not yet been confirmed due to the lack of sufficient evidence.[39] In order to get more information about the origin of this kind of resistance drop, we carried out electrical transport measurements at varying temperatures under magnetic fields. The $R(T)$ data of $La_2NiO_{4.06}$ under 0 T, 1 T, and 9 T magnetic fields are depicted in Fig. 3(c). The results show that the transition temperature under 1 T and 9 T is basically the same as that under 0 T, and there is no evidence of transition temperature suppression by magnetic field. In addition, for $T > T_{IMT}$, there is a weak negative magnetoresistance effect at 1 T, and the resistance does not continue to decrease at 9 T, showing saturation magnetoresistance behavior. We note that there is a bulge appearing in the $R(T)$ curve under 9 T around 165 K, which is highly close to the previously reported magnetic order transition temperature ($\sim$170 K) in $La_2NiO_4$, indicating that it may originate from the coupling of electrical transport property and magnetic order transformation[40–42] under high

magnetic field. Overall, the external magnetic field affects the electrical transport behavior to a certain extent, but does not inhibit the low-temperature resistance drop phenomenon.

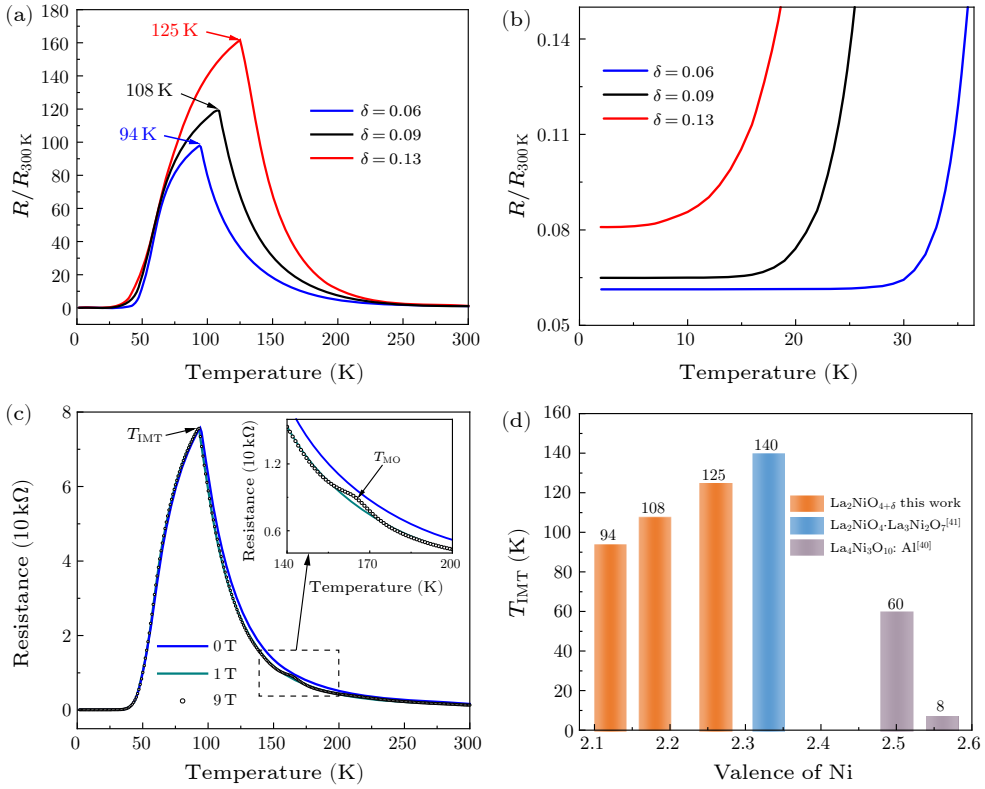


**Fig. 3.** Non-superconducting metallic ground state in $La_2NiO_{4+\delta}$ single crystals. (a) Temperature dependence of the resistivity normalized to the resistivity at 300 K. (b) Enlarged view of the low temperature region in (a). (c) Temperature dependence of resistance of $La_2NiO_{4.06}$ at ambient pressure under magnetic fields of 0 T, 1 T, and 9 T. No magnetic-field suppression effect on the resistivity transition exists. An enlarged view of the resistance bulge under high magnetic fields is shown in the upper right inset. (d) The insulator-to-metal transition temperature $T_{IMT}$ as a function of the valence of Ni in RP phase lanthanum nickelates.

In short, based on the lack of both zero-resistance and transition temperature suppression by external magnetic field, which are common criteria for superconductivity, the resistance decrease behavior at low temperature found in $La_2NiO_{4+\delta}$ cannot be ascribed as superconductivity. Here, we attribute this phenomenon to an insulator-to-metal transition (IMT). It is worth noting that similar IMT behaviors under low temperature were also observed in other RP phase Lanthanum nickelates, such as Al-doped $La_4Ni_3O_{10}$,[43] and recently synthesized three-dimensional hybridization $La_2NiO_4{\cdot}La_3Ni_2O_7$.[44] Although a variety of mechanisms have been proposed, the IMT transition remains one of the least understood phenomena in condensed matter physics systems.[45] Discovering commonalities between samples with this phenomenon is crucial to gaining insight into the nature. Note that the interstitial oxygen, electronic doping, and structural hybridization all change the valence of Ni ($V_{Ni}$) in lanthanum nickelates. The relationship between $T_{IMT}$ and $V_{Ni}$ (calculated based on charge balance) is summarized in Fig. 3(d). Intriguingly, $T_{IMT}$ first increases and then decreases with the augment of $V_{Ni}$, and has a maximum value near $V_{Ni}$ ($T_{IMT}$ max) = 2.33, showing a dome shape. It is worth noting that the highest superconducting transition temperature in lanthanum nickelates is currently achieved in $La_3Ni_2O_{7-\delta}$ ($\delta = 0.07$), which corresponds to $V_{Ni}$ ($T_c$ max) = 2.43. The high proximity of $V_{Ni}$ ($T_c$ max) and $V_{Ni}$ ($T_{IMT}$ max) in lanthanum nickelates implies that the valence state of Ni may plays an important role in the electronic ground state of lanthanum nickelates.

Pressure is an alternative method to modulate physical properties beyond chemical doping and external magnetic fields, and can provide important information about the evolution of electronic states without changing the chemical composition. To the best of our knowledge, there are few studies reported on the effect of pressure on IMT happened at low temperatures. In order to gain a deeper understanding of the novel metallic ground state, we measured $R(T)$ curves of $La_2NiO_{4+\delta}$ single crystals under pressure, and the results are shown in Figs. 4(a), 4(b), and 4(c). It is found that the $T_{IMT}$ values of these samples exhibit the same high-pressure behavior: as the pressure increases, $T_{IMT}$ persistently decreases, when it reaches the critical pressure, marked as $P_c$ (about 13.1, 26.1, 35.6 GPa, for $\delta = 0.06$, 0.09, 0.13, respectively), IMT disappears, indicating that the samples enter an insulating ground state from the metallic ground state. We summarized the experimental results in the temperature-pressure phase dia-

grams (see Fig. S3 in the Supplementary Material), from which we can intuitively find that the metallic-like state is located in the low-temperature and low-pressure region, the insulating state is located in the high-temperature and high-pressure region, and the middle is the high resistance area (marked in red) where the IMT occurs. It is worth noting that $T_{\rm IMT}$ and $P_{\rm c}$ show a similar positive dependence on oxygen content [Fig. 4(d)]. These results indicate that the factors that determine the thermal stability ($T_{\rm IMT}$) and quantum stability ($P_{\rm c}$) of the novel metallic ground states in $La_2NiO_{4+\delta}$ are similar.

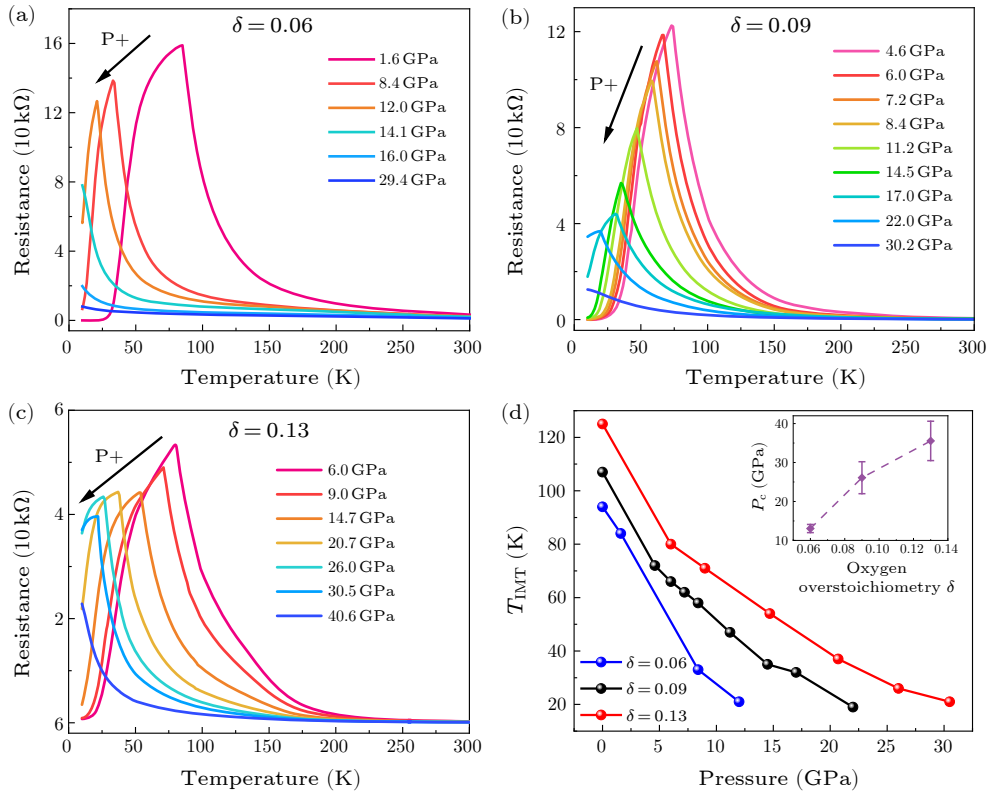


**Fig. 4.** The high-pressure suppression effect on the insulator-to-metal transition of $La_2NiO_{4+\delta}$. [(a), (b), (c)] Temperature dependence of resistivity $R(T)$ for $La_2NiO_{4+\delta}$ single crystals under pressure with $\delta = 0.06$, 0.09, and 0.13, respectively. (d) Dependence of the insulator-to-metal transition temperature ($T_{\rm IMT}$) and the metallic-to-insulating ground state transition pressure ($P_{\rm c}$) on oxygen overstoichiometry $\delta$.

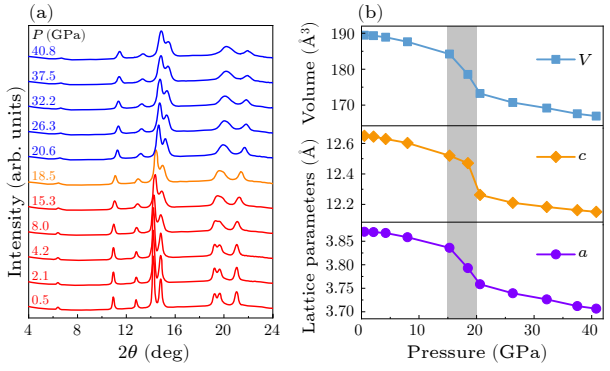


**Fig. 5.** Isostructural phase transition of $La_2NiO_{4.06}$ under pressure. (a) Pressure dependence of XRD pattern. The x-ray wavelength is 0.709 Å. (b) Evolution of the lattice parameters $a$ and $c$ and the unit-cell volume $V$ with pressure.

High-pressure x-ray diffraction is used to study the structural origin of the disappearance of metallic ground states under pressure. The measurement results of $La_2NiO_{4.06}$ are shown in Fig. 5(a). As the pressure increases, the peaks gradually move to higher angles. Up to 40.2 GPa, the XRD patterns can be well described by the ambient structure with $I4/mmm$ space group (see Fig. S4) and the goodness-of-fit parameters are $R_{\rm wp} = 1.77\%$ and $R_{\rm P} = 1.56\%$. The evolution of lattice parameters and unit-cell volume with pressure obtained by Rietveld fitting are shown in Fig. 5(b). Both the lattice parameters $a$ and $c$ show a discontinuous decrease around 15–20 GPa, resulting in a sudden shrinkage of the unitcell volume, indicating that the phase change is of first order. Similar isostructural phase transitions at high pressure are also observed in $La_2NiO_{4.09}$ and $La_2NiO_{4.13}$ (see Fig. S6), and the transition pressure increases with the increase of oxygen content (see Fig. S7), which is qualitatively consistent with the electrical measurement results. Therefore, the transition from the metallic ground state to insulating ground state in $La_2NiO_{4+\delta}$ could be tentatively attributed to the isostructural phase transition under pressure.

In summary, we have unveiled a novel insulator-to-metal transition in $La_2NiO_{4+\delta}$ synthesized through crucible-free floating-zone method combined with post-

annealing treatment. Absence of zero-resistance and magnetic-field suppression effects on the transition temperature excludes the possibility of superconductivity. In addition, compared to the weak magnetic-field effects, pressure can significantly suppress the transition and transform from the metallic to an insulating ground state, accompanied by an isostructural phase transition. Our work provides insights into the long-elusive metallic conductive ground state in $La_2NiO_{4+\delta}$ and contributes to understand the puzzle of high-temperature superconductivity in single-layer lanthanum nickelates.

*Acknowledgments.* This work was supported by the National Key Research and Development Program of China (Grant No. 2023YFF0804100), the National Natural Science Foundation of China (Grant Nos. 12274168, 12074141, and 42102030), Jilin Provincial Science and Technology Development Project (Grant Nos. 20210402054GH and 20220101011JC), and the Program for Jilin University Science and Technology Innovative Research Team (Grant No. 2021-TD-05). We acknowledge the support from the Fundamental Research Funds for the Central Universities, and National Major Science Facility Synergetic Extreme Condition User Facility Achievement Transformation Platform Construction (Grant No. 2021FGWCXNLJSKJ01).

## References

[1] Anisimov V I, Bukhvalov D, and Rice T M 1999 *Phys. Rev. B* **59** 7901
[2] Zachar O, Kivelson S A, and Emery V J 1998 *Phys. Rev. B* **57** 1422
[3] Lechermann F 2020 *Phys. Rev. B* **101** 081110
[4] Li D, Lee K, Wang B Y, Osada M, Crossley S, Lee H R, Cui Y, Hikita Y, and Hwang H Y 2019 *Nature* **572** 624
[5] Zeng S, Li C J, Chow L E, Cao Y *et al.* 2022 *Sci. Adv.* **8** eabl9927
[6] Gu Q Q and Wen H H 2022 *Innovation* **3** 100202
[7] Wu X, Di Sante D, Schwemmer T, Hanke W, Hwang H Y, Raghu S, and Thomale R 2020 *Phys. Rev. B* **101** 060504
[8] Hou J, Yang P T, Liu Z Y, Li J Y, Shan P F, Ma L, Wang G, Wang N N, Guo H Z, Sun J P, Uwatoko Y, Wang M, Zhang G M, Wang B S, and Cheng J G 2023 *Chin. Phys. Lett.* **40** 117302
[9] Sun H, Huo M, Hu X *et al.* 2023 *Nature* **621** 493
[10] Wang G, Wang N N, Shen X L, Hou J, Ma L, Shi L F, Ren Z A, Gu Y D, Ma H M, Yang P T, Liu Z Y, Guo H Z, Sun J P, Zhang G M, Calder S, Yan J Q, Wang B S, Uwatoko Y, and Cheng J G 2024 *Phys. Rev. X* **14** 011040
[11] Shen Y, Qin M P, and Zhang G M 2023 *Chin. Phys. Lett.* **40** 127401
[12] Jiang K, Wang Z, and Zhang F C 2024 *Chin. Phys. Lett.* **41** 017402
[13] Wang M, Wen H H, Wu T, Yao D X, and Xiang T 2024 *Chin. Phys. Lett.* **41** 077402
[14] Zhu Y *et al.* 2024 *Nature* **631** 531
[15] Sakakibara H, Ochi M, Nagata H, Ueki Y, Sakurai H, Matsumoto R, Terashima K, Hirose K, Ohta H, Kato M, Takano Y, and Kuroki K 2024 *Phys. Rev. B* **109** 144511
[16] Li Q, Zhang Y J, Xiang Z N, Zhang Y, Zhu X, and Wen H H 2024 *Chin. Phys. Lett.* **41** 017401
[17] Zhang M, Pei C, Du X *et al.* 2023 arXiv:2311.07423 [cond-mat.supr-con]
[18] Thanh T D, Van H T, Thu D T A, Bau L V, Van Dang N, Nam D N H, Hong L V, and Yu S C 2017 *IEEE Trans. Magn.* **53** 8204904
[19] Burns G, Dacol F H, Rice D E, Buttrey D J, and Crawford M K 1990 *Phys. Rev. B* **42** 10777
[20] Jorgensen J D, Dabrowski B, Pei S Y, Richards D R, and Hinks D G 1989 *Phys. Rev. B* **40** 2187
[21] Kąkol Z,, Spałek J, and Honig J M 1989 *J. Solid State Chem.* **79** 288
[22] Kąkol Z, Spałek J, and Honig J M 1989 *Solid State Commun.* **71** 283
[23] Nanjundaswamy K S, Lewicki A, Kakol Z, Gopalan P, Metcalf P, Honig J M, Rao C N R, and SpaŁek J 1990 *Physica C* **166** 361
[24] Acrivos J V, Lei M C, Jiang C, Nguyen H, Metcalf P, and Honig J M 1994 *J. Solid State Chem.* **111** 343
[25] Ganguli A K, Nagarajan R, Rao G R, Vasanthacharya N Y, and Rao C N R 1989 *Solid State Commun.* **72** 195
[26] Spałek J, Kąkol Z, and Honig J M 1989 *Solid State Commun.* **71** 511
[27] Poirot N, Odier P, Simon P, and Gervais F 2003 *Solid State Sci.* **5** 735
[28] Saleem M, Singh D, Mishra A, and Varshney D 2019 *Mater. Res. Express* **6** 026304
[29] Zhou N, Chen G, Zhang H J, and Zhou C 2009 *Physica B* **404** 4150
[30] Sayer M and Odier P 1987 *J. Solid State Chem.* **67** 26
[31] Vashook V V, Trofimenko N E, Ullmann H, and Makhnach L V 2000 *Solid State Ionics* **131** 329
[32] Zhang M, Pei C, Wang Q, Zhao Y, Li C, Cao W, Zhu S, Wu J, and Qi Y 2024 *J. Mater. Sci. Technol.* **185** 147
[33] Hosoya T, Igawa K, Takeuchi Y, Yoshida K, Uryu T, Hirabayashi H, and Takahashi H 2008 *J. Phys.: Conf. Ser.* **121** 052013
[34] Gao R, Jin L, Huyan S, Ni D, Wang H, Xu X, Bud'ko S L, Canfield P, Xie W, and Cava R J 2024 *ACS Appl. Mater. Interfaces*
[35] Rice D E and Buttrey D J 1993 *J. Solid State Chem.* **105** 197
[36] Hücker M, Chung K, Chand M, Vogt T, Tranquada J M, and Buttrey D J 2004 *Phys. Rev. B* **70** 064105
[37] Udagawa M, Yamaguchi T, Nagaoka Y, Ogita N, Kato M, Maeno Y, Fujita T, and Ohbayashi K 1993 *Phys. Rev. B* **47** 11391
[38] Bates F E and Eldridge J E 1989 *Solid State Commun.* **72** 187
[39] Zhou X, Qin P, Feng Z, Yan H, Wang X, Chen H, Meng Z, and Liu Z 2022 *Mater. Today* **55** 170
[40] Wu G and Neumeier J J 2003 *Phys. Rev. B* **67** 125116
[41] Nikonov A A and Parfenov O E 2003 *J. Exp. Theor. Phys. Lett.* **78** 25
[42] Wochner P, Tranquada J M, Buttrey D J, and Sachan V 1998 *Phys. Rev. B* **57** 1066
[43] Periyasamy M, Patra L, Fjellvåg Ø S, Ravindran P, Sørby M H, Kumar S, Sjåstad A O, and Fjellvåg H 2021 *ACS Appl. Electron. Mater.* **3** 2671
[44] Li F Y, Guo N, Zheng Q, Shen Y, Wang S L, Cui Q H, Liu C, Wang S P, Tao X T, Zhang G M, and Zhang J J 2024 *Phys. Rev. Mater.* **8** 053401
[45] Mott N F 1968 *Rev. Mod. Phys.* **40** 677